Journal of Engineering Physics and Thermophysics, Vol. 70, No. 6, 1997

RESISTANCE REDUCTION AND STABILITY IMPROVEMENT FOR HELICOPTER-SHIPPED LOADS WHEN A LEADING SEPARATION ZONE IS ORGANIZED

S. A. Isaev and N. A. Sumovskii

UDC 532.517.4

Based on flight tests in shipment by helicopters and numerical modeling of flow along parallelepiped-like loads the authors analyze the resistance reduction and stability improvement for the motion of a blunt body with vertical stabilizers when a leading separation zone is organized.

1. Very rigid requirements, in both the context of flight safety and economic efficiency, are imposed on suspended load shipment by helicipters of various types. It should be noted that the mass of the loads can attain 20 tons and their major portion is constituted by the objects like small houses and containers, i.e., blunt bodies and loads in the form of parallelepipeds. Suspended load shipment leads to serious difficulties since there is a tendency for progressive oscillations of the loads as the helocopter's flying speed increases. Helicopters of the Mi-6T and Mi-10K types are known to have crashed while shipping bulk loads. Thus, substantial restrictions are imposed on the cruising flight speed for suspended-load helicopters. Usually it is about 60–80 km/h, which makes economic indexes much worse (speeds of about 170–200 km/h are the most efficient).

The indicated complicated typically operational problem is within the framework of the known concept of controlling the flow along bodies by purposive flow separation [1]. In this case, we consider a combination of the method of stabilization by a rudder unit, which became classical in aviation, with the nontraditional but very promising front stabilization, when a baffle is placed in front of the body. In addition to front stabilization, aerodynamic resistance is reduced, which has been fairly well studied for flow along cylindrical bodies with coaxial disks [2, 3].

This work seeks to investigate means of stabilization and reduction of the resistance of loads with a three-dimensional configuration with the aim of increasing the safe speed of helicopter shipment of suspended loads. Means of stabilization and resistance reduction (vertical–stabilizer dimensions, the dimensions of the front plate as well as the gap between the plate and the end surface of the load) are chosen based on the results of physical and numerical experiments. The static aerodynamic coefficients C_x, C_y, C_z, M_z, etc. are calculated on personal computers. Dynamic characteristics of the considered bodies are determined in tests of the models in wind tunnels of the Riga Experimental Center of the State Scientific-Research Institute of Civil Aviation. A numerical investigation of the pattern of flow along loads is oriented to obtaining information on the controlling physical mechanisms and on the evolution of the flow structure when the angles of attack and slip are increased.

The object of the investigation was a parallelepiped cottage with installed front and tail stabilizers and resistance reduction. Two vertical rectangular plates are used as vertical stabilizers. The device for front stabilization and simultaneous drag reduction is a rectangular baffle of a certain size fixed at a specified distance from the front surface of the parallelepiped. Flight tests of suspended loads are performed at speeds of 0 to 250 km/h.

Deformation of the vortex structure in the body's front at nonzero angles of attack and slip contributes to the occurrence of a restoring moment that stabilizes the load during a flight. The use of the additional vertical stabilizers ensures load stability in shipment.

Academy of Civil Aviation, St. Petersburg. Translated from Inzhenerno-Fizicheskii Zhurnal, Vol. 70, No. 6, pp. 990-995, November-December, 1997. Original article submitted October 30, 1995.

 1062-0125/97/7006-0952$18.00

2. As is well known [2-4], the organization of large-scale vortex structures for the flow along blunt bodies by the purposive separation of the flow on thin disks in front of the bodies and behind them enables us to substantially improve their aerodynamic characteristics, leading not only to a reduction in the drag but also to stability improvement owing to the effect of front stabilization. Preliminary investigations of this problem [1] are concerned with the detailed analysis of the effect of the reduction in the drag of the bodies of this nontraditional geometry. It is shown that, for subsonic flow velocities, the profile resistance of a cylinder with a flat end can be decreased by a factor of 50–100 because of a thin disk of the specified diameter is installed at a certain distance in front of it and can be compared with the profile resistance of cylinders with a semispherical point. Similarly, the bottom resistance of a body with a disk at the bottom can be decreased by a factor of 1.5–2 as compared to the bottom resistance of the body without a disk [3]. Moreover, for significantly long cylinders, it proves possible to reduce the drag by decreasing the viscous friction resistance [1].

The performed numerical investigation of vortex flow along three-dimensional bodies of complex geometry is based on known mathematical models that depend on solution of a system of Reynold equations for turbulent flow of an incompressible viscous fluid. To close the system, we used a high-Reynolds version of a two-parametric dissipative turbulence model in combination with a widely tested method of wall functions. This approach is suitable for modeling fully developed turbulent flows. It is tested for problems of circulation flow in a cavity and in a near wake behind a disk, detached flow along two coaxial disks, and a combination of a cylinder with a protruding disk, for which the obtained numerical results are compared with the experimental data of Miles, Carmodi, Morel and Bon, Roshko and Kenig, Below and Isaev as well as with other results of turbulent-flow calculations on the basis of a more complicated algebraic version of the multiparametric model of Reynolds stresses that is proposed by Rodi.

The initial equations in dimensionless form for the generalized variable $\varphi = (u, v, w, k, \varepsilon)$ in curvilinear nonorthogonal coordinates ξ, η, and ζ have the form

$$(U\varphi)_\xi + (V\varphi)_\eta + (W\varphi)_\zeta = \left[\frac{\Gamma^\varphi}{J}(D_{11}^2 + D_{12}^2 + D_{13}^2)\varphi_\xi\right]_\xi +$$

$$+ \left[\frac{\Gamma^\varphi}{J}(D_{21}^2 + D_{22}^2 + D_{23}^2)\varphi_\eta\right]_\eta + \left[\frac{\Gamma^\varphi}{J}(D_{31}^2 + D_{32}^2 + D_{33}^2)\varphi_\zeta\right]_\zeta + S^\varphi J .$$

Here the indexes ξ, η, and ζ are the derivatives along the indicated coordinate vectors. The source terms S^φ, in addition to the source and runoff components proper, involve diffusion terms that are due to the nonorthogonality of the chosen coordinate system S_{ob}^φ (the subscript ob denotes an oblique angle). The latter are expressed in the following manner:

$$S_{ob}^\varphi = \frac{1}{J}\left[\frac{\Gamma^\varphi}{J}(D_{11}D_{21} + D_{12}D_{22} + D_{13}D_{23})\varphi_\eta + \frac{\Gamma^\varphi}{J}(D_{11}D_{31} + D_{12}D_{32} + D_{13}D_{33})\varphi_\zeta\right]_\xi +$$

$$+ \frac{1}{J}\left[\frac{\Gamma^\varphi}{J}(D_{11}D_{21} + D_{12}D_{22} + D_{13}D_{23})\varphi_\xi + \frac{\Gamma^\varphi}{J}(D_{21}D_{31} + D_{22}D_{32} + D_{23}D_{33})\varphi_\zeta\right]_\eta +$$

$$+ \frac{1}{J}\left[\frac{\Gamma^\varphi}{J}(D_{11}D_{31} + D_{12}D_{32} + D_{13}D_{33})\varphi_\xi + \frac{\Gamma^\varphi}{J}(D_{21}D_{31} + D_{22}D_{32} + D_{23}D_{33})\varphi_\eta\right]_\zeta .$$

The source components that are governed by a pressure gradient are represented as

$$S_p^\varphi = \frac{1}{J}(p_\xi D_{1j} + p_\eta D_{2j} + p_\zeta D_{3j}) ,$$

where $j = 1, 2, 3$ correspond to the equations for u, v, and w.

The remaining source terms for the j-th momentum equation are written as

$$S_j^{\varphi} = \frac{1}{J}\left[\frac{\Gamma^{\varphi}}{J}(D_{11}u_{\xi} + D_{12}v_{\xi} + D_{13}w_{\xi})\,D_{1j} + \frac{\Gamma^{\varphi}}{J}(D_{11}u_{\eta} + D_{12}v_{\eta} + D_{13}w_{\eta})\,D_{2j} + \right.$$

$$\left. + \frac{\Gamma^{\varphi}}{J}(D_{11}u_{\zeta} + D_{12}v_{\zeta} + D_{13}w_{\zeta})\,D_{3j}\right]_{\xi} + \frac{1}{J}\left[\frac{\Gamma^{\varphi}}{J}(D_{21}u_{\xi} + D_{22}v_{\xi} + D_{23}w_{\xi})\,D_{1j} + \right.$$

$$\left. + \frac{\Gamma^{\varphi}}{J}(D_{21}u_{\eta} + D_{22}v_{\eta} + D_{23}w_{\eta})\,D_{2j} + \frac{\Gamma^{\varphi}}{J}(D_{21}u_{\zeta} + D_{22}v_{\zeta} + D_{23}w_{\zeta})\,D_{3j}\right]_{\eta} +$$

$$+ \frac{1}{J}\left[\frac{\Gamma^{\varphi}}{J}(D_{31}u_{\xi} + D_{32}v_{\xi} + D_{33}w_{\xi})\,D_{1j} + \frac{\Gamma^{\varphi}}{J}(D_{31}u_{\eta} + D_{32}v_{\eta} + D_{33}w_{\eta})\,D_{2j} + \right.$$

$$\left. + \frac{\Gamma^{\varphi}}{J}(D_{31}u_{\zeta} + D_{32}v_{\zeta} + D_{33}w_{\zeta})\,D_{3j}\right]_{\zeta}.$$

It is significant that the source terms that are written above are formulated in divergent form, which enables us to construct a conservative computational scheme.

The countervariant variables U, V, and W that are responsible for convective transfer through the edges of cells are determined as:

$$U = D_{11}u + D_{12}v + D_{13}w, \quad V = D_{21}u + D_{22}v + D_{23}w, \quad W = D_{31}u + D_{32}v + D_{33}w.$$

The metric coefficients D_{ij} and the Jacobian J that appear in the above equations are functions of the Cartesian coordinates x, y, and z:

$$D_{ij} = \begin{vmatrix} y_{\eta}z_{\zeta} - y_{\zeta}z_{\eta} & x_{\zeta}z_{\eta} - x_{\eta}z_{\zeta} & x_{\eta}y_{\zeta} - x_{\zeta}y_{\eta} \\ y_{\zeta}z_{\xi} - y_{\xi}z_{\zeta} & x_{\xi}z_{\zeta} - x_{\zeta}z_{\xi} & x_{\zeta}y_{\xi} - x_{\xi}y_{\zeta} \\ y_{\xi}z_{\eta} - y_{\eta}z_{\xi} & x_{\eta}z_{\xi} - x_{\xi}z_{\eta} & x_{\xi}y_{\eta} - x_{\eta}y_{\xi} \end{vmatrix},$$

$$J = x_{\xi}y_{\eta}z_{\zeta} + x_{\zeta}y_{\xi}z_{\eta} + x_{\eta}y_{\zeta}z_{\xi} - x_{\xi}y_{\zeta}z_{\eta} - x_{\eta}y_{\zeta}z_{\xi} - x_{\zeta}y_{\eta}z_{\xi}.$$

Discretization of the controlling differential equations is realized within the framework of the concept of splitting by physical processes using the finite-volume method, which is applied to the equations written in increments in dependent variables in the so-called E-factor formulation [1].

To ensure high accuracy of calculations in the special cases that, in the flow field, there form zones with large gradients of the parameters which govern flow, we use Leonard's counterflow quadratic-interpolation scheme of low circuit diffusion to approximate the convective terms in the explicit side of the equations. At the same time, to improve computational stability and to damp possible nonphysical oscillations, in the numerical solution we use the counterflow scheme of the first-order approximation in combination with the introduction of additional diffusion in the implicit side of the transport equations.

High efficiency of calculations is ensured not only by the use of Buleev's method of incomplete matrix factorization to solve the finite-difference equations. In the pressure-correction unit, we use the matched SIMPLEC computational procedure, which enables us to avoid lower relaxation in the iteration process of determination of a pressure correction, which is characteristic of the traditional SIMPLE approach. The increase in efficiency is also attributed to the use of the Rhi–Chou method, in which a monotonizer is introduced to damp pressure-correction oscillations on a centered net with unbiased nodes. The unit of initial-data preparation contains a generator of curvilinear nonorthogonal nets that are matched with boundaries. Computational nets are constructed numerically using automated arrangement of nodes on the basis of the solution of elliptical-type differential equations and using algebraic procedures.

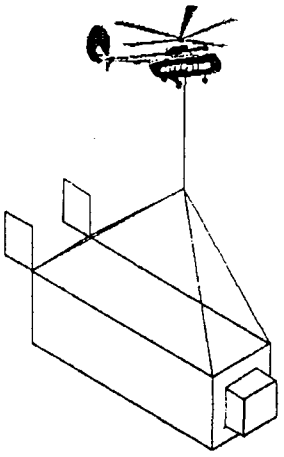

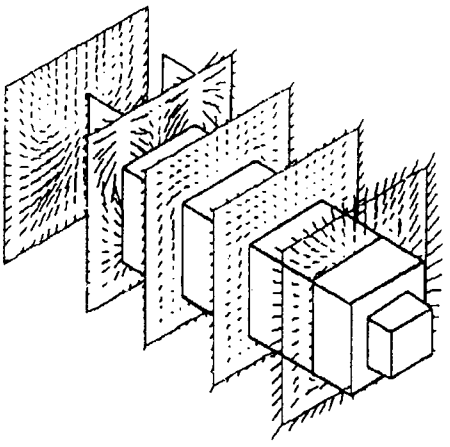

Fig. 1. Aerodynamic arrangement of suspended load in helicopter with stabilization and drag reduction.

Fig. 2. Secondary-flow pattern in cross-sections of the design domain for flow along a load at zero angles of attack and slip.

The developed codes are tested by solving partial problems in which different governing factors are taken in account separately. Each package is verified based on comparison of the numerical results with the available data of reliable physical experiments and other numerical results that are obtained by different computational methods. Some traditional (as for the known PHOENICS, FIDAP, FIRE, and FLOW 3D packages) features such as friendliness of the developed interface, interactive graphics, context support, mobility and simplicity in reproduction when further modifications are performed, etc. are inherent in the developed codes.

The designed software is an efficient tool for a numerical investigation of the mechanism of front stabilization for bodies of revolution of small elongation in the presence of a protruding disk. The efficiency of the nontraditional approach to the stability of body motion is estimated by comparison of the aerodynamic characteristics for blunt bodies with installed protruding disks and vertical stabilizers. We also formulate some practical recommendations on the choice of aerodynamic arrangements that are efficient as far as the criteria of safety and operating efficiency are concerned as applied to suspended load stability.

Some numerical and experimental results obtained are presented in Figs. 1-4. The object of investigation of Fig. 1 is oriented with respect to the incoming flow at different angles of attack and slip that range from 0 to 10°. The computational net contained about 30,000 nodes that were nonuniformly distributed throughout the space around the load model with thickening in the vicinity of the body, the plate ahead, and tailplanes. To simplify the geometry of the object of investigation, in numerical calculations, the plate in front of the load is replaced by a parallelepiped-type protrusion. This approach seems to be quite justified, since a similar approach to axisymmetric step bodies [5] reveals quite acceptable results when an arrangement with the bodies that are separated by a gap is replaced by a step body. The geometric dimensions of the protrusion (see Fig. 1) correspond to the configuration of the front separation zone, which makes it possible to decrease the body's drag to the largest extent, as follows from physical experiments in wind tunnels. The Reynolds number in the calculations was taken to correspond to the tunnel experiment and to be 10^7.

The pattern of flow along the load at zero angles of attack and slip of Fig. 2 reveals vortex structures in the near wake which are typical of similar bodies and form as a result of vortex curtain turning. Organization of the front separation zone leads to a smooth character of the flow along an angular body, as a parallelepiped, similar to the flow along a cylinder with a protruding disk.

The influence of the angles of attack α and slip β on the deformation of the pressure fields near step bodies illustrates the effect of front stabilization of bodies with a forward separation zone (Fig. 3). For nonzero angles of attack and slip, the asymmetry of flow along the body leads to the occurrence of the restoring moment (for example, $M_y(\beta) < 0$).

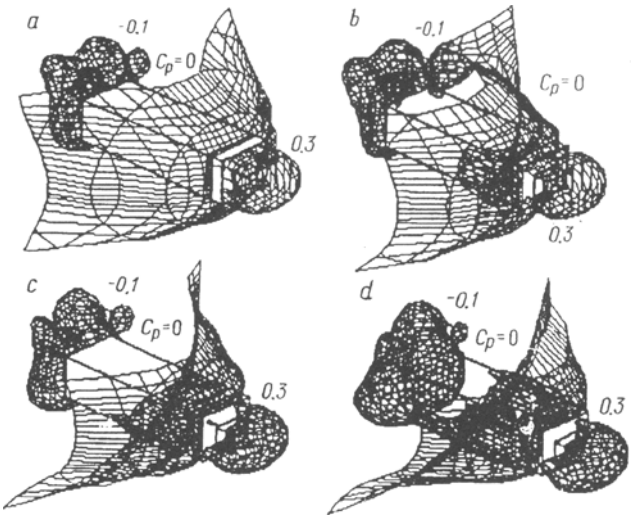

Fig. 3. Influence of the angles of attack and slip on deformation of the pressure field in the vicinity of a parallelepiped with a rectangular protrusion and vertical stabilizers in a uniform flow: a) $\alpha = 0, \beta = 0$; b) $\alpha = 0, \beta = 5^{\circ}$; c) $\alpha = 5^{\circ}, \beta = 5^{\circ}$; d) $\alpha = 5^{\circ}, \beta = 10^{\circ}$.

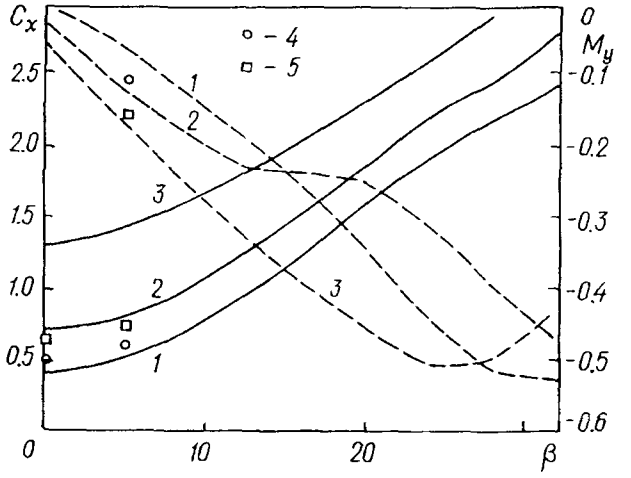

Fig. 4. Drag coefficient C_x (solid lines) and restoring moment M_y (dashed lines) as functions of the angles of attack α and slip β: 1, 2, and 3) experiment, $\alpha = 0$, 5, and 10 °, respectively; 4 and 5) calculation, $\alpha = 0$ and 5°, respectively.

The comparative analysis of aerodynamic characteristics for a body of optimum geometry with an elongation of 3 calibers (of the cross dimensions of a parallelepiped) that is performed in Fig. 4 based on the results of numerical modeling and these wind-tunnel tests shows that numerical predictions seem quite satisfactory.

3. At the All-Union Scientific-Research Institute for Applying Aviation to the National Economy, the experimental equipment is designed and produced, and using it, flight tests of 2.8 × 2.5 × 8 m small houses with a mass of 7000 kg are performed. A small house was shipped on an external suspension of an Mi-26 helicopter equipped with measuring and recording devices for the angular coordinates of load and the flight speed. Analysis was made of the following variants of flights with the house: a) without a front plate or stabilizers; b) with a front plate but without stabilizers; c) without a front plate but with stabilizers; d) with a front plate and stabilizers. In the latter variant, three different distances between the plate and the house are considered: a distance that is smaller than the optimum one, the optimum distance, and a distance that is larger than the optimum one. The optimum gap between the plate and the house is determined using numerical modeling and wind-tunnel tests; it corresponded to the local minimum drag of the arrangement. The procedure of each flight test involved a successive

increase of over 60 km/h in the speed with a step of 20 km/h with a 1-minute holding of the speed. When the speed approaches its maximum for this variant the step decreases. The minimum speed for each flight was determined twice in forward and backward directions to eliminate the influence of wind.

The resultant maximum speeds for external shipment of the houses in the flight tests were as follows: a) without a front plate and without stabilizers – 90 km/h; b) with a front plate but without the stabilizers – 130 km/h; c) without a front plate but with stabilizers – 140 km/h; d) with a front plate and with stabilizers when the gap is smaller than the optimum one – 155 km/h, for the optimum gap – 235 km/h, for a gap that is larger than the optimum one – 130 km/h. The obtained results permit an increase of 2.5 times in the safe speed for shipment of suspended loads in the form of a parallelepiped.

The work was carried out with financial support from the Russian Fundamental Research Fund, grant No. 95-01-00728.

NOTATION

x, y, and z, Cartesian coordinates; ξ, η, ζ, curvilinear nonorthogonal coordinates; u, v, and w, Cartesian velocity components; U, V, and W, countervariant variables; p, static pressure referred to the doubled velocity head of the incoming flow; k, turbulence energy; ε, rate of turbulent energy dissipation; φ, generalized dependent variable; Γ^{φ}, diffusive transport coefficient; J, Jacobian; D_{ij}, tensor of metric coefficients; S^{φ}, source term in the transport equation; S_j^{φ}, source term in the j-th momentum equation due to diffusive transfer; S_p^{φ}, source term due to the pressure gradient; S_{0b}^{φ}, source term due to the oblique-angled nature of the coordinate system; Re, Reynolds number; α, angle of attack; β, angle of slip; $M_y(\beta)$, restoring moment that is made dimensionless by means of the velocity head and midship-section area of load; C_x, drag coefficient that is made dimensionless by means of the velocity head and midship-section area; C_p, pressure coefficient.

REFERENCES

1. I. A. Belov, S. A. Isaev, and V. A. Korobkov, Problems and Calculation Methods for Detached Flows of Incompressible FLuids [in Russian], Leningrad (1989).
2. V. K. Bobyshev and S. A. Isaev, Inzh.-Fiz. Zh., 58, No. 4, 556-572 (1990).
3. S. A. Isaev, Inzh.-Fiz. Zh., 68, No. 1, 19-25 (1995).
4. I. A. Belov, V. K. Bobyshev, and S. A. Isaev, Investigations of Aerodynamics and Flight Dynamics [in Russian], Kiev (1988), pp. 122-129.
5. S. A. Isaev, V. M. Suprun, and O. A. Shul'zhenko, Inzh.-Fiz. Zh., 80, No. 3, 433-439 (1991).